

# Impact of Relays and Supporting Nodes on Locally Restricted Cooperation in Future Cellular Networks

Michael Kuhn, University of Applied Sciences, Darmstadt, Germany  
Raphael Rolny, and Marc Kuhn, ETH Zurich, Switzerland  
michael.kuhn@h-da.de, {rolny, kuhn}@nari.ee.ethz.ch

**Abstract**—In this paper, we compare different locally restricted cooperation schemes for the downlink of LTE-Advanced. The focus in our investigations is on schemes which are easy to implement and thus have a high level of practical relevance. Two different optimization goals are considered. We first investigate how a target data rate can be achieved with lowest transmit (Tx) power. Reduction of Tx power will lead to reduced electromagnetic radiation as well as lower total power consumption of the eNodeBs. Furthermore, it will result in reduced interference between adjacent cooperation sets. We secondly maximize the data rate that can be achieved by different schemes for fixed Tx power while considering fairness between the users. Additionally, we consider implementation issues and give an estimation of achievable data rates in case of limited backhaul capacity of practical 4G networks.

## I. INTRODUCTION

The ITU requirements for IMT-Advanced demand peak data rates of up to 1 Gbit/s in 4G networks as LTE-Advanced [1]. Although the bandwidth of LTE-Advanced will be much higher compared to 3G networks, the transmit power cannot be increased by the same amount. With existing sites and locally independent transmission schemes it will be difficult to achieve these high data rates, especially at cell edges [2]. However, finding new sites for base stations (also called eNodeBs) is already becoming an increasing problem for many operators due to resident's sensibility and anxiety of electromagnetic radiation and electromagnetic fields.

Recent research results [3] show that cooperation schemes in the downlink of 4G are able to solve many of the issues faced by future cellular networks. Such cooperative schemes can include cooperation among several eNodeBs, among several sectors of one eNodeB or between mobile user equipments (UEs), in order to form distributed multiple-input multiple-output (MIMO) arrays to achieve a higher spectral efficiency. LTE-Advanced standardizes coordinated multipoint (CoMP) transmission and reception to achieve such network MIMO gains. Coordinated multipoint transmission for the downlink means dynamic coordination among transmitting eNodeBs, like joint beamforming to the same mobile. However, in real networks the number of cells is too high to consider all eNodeBs in one cooperation scheme. The computational complexity and the requirements on delay can then hardly be met. As a consequence, cooperation has to be limited to a subset of eNodeBs. Only eNodeBs of one subset will cooperate, all other eNodeBs have to be considered as interference.

In this paper we investigate CoMP schemes which use

low-power nodes and compare them to cooperative schemes presented in [3]. We distinguish between three different types of low-power nodes: Supporting nodes which can be understood as remote radio heads, femto-cells which use an additional transmission standard, and relays, sharing the frequency resources of the mobile network. In contrast to [3], the focus of this paper is not only on maximizing data rates, but also on minimization of transmission power. Furthermore, we consider limitations of the backhaul capacity. Our results deliver important insights into future cell planning aspects.

## II. SYSTEM MODEL

In our non-cooperative *reference scenario* we assume an area divided into cells of hexagonal shape. Each cell has a radius of 350m and consists of equally formed and sized sectors. For the reference scenario, the eNodeB is placed in the center of the cell. In order to avoid co-channel interference, the sectors of one cell are separated by different carrier frequencies (frequency reuse factor 3). The setup is depicted in Figure 1(a). Note that this corresponds to a typical setup used in current cellular networks. The different sectors of one eNodeB as well as different eNodeBs work independently from each other, i.e. no cooperation between different sectors or different eNodeBs is performed. The eNodeB is equipped with sectorized 120 degree directional antennas, each consisting of four antenna elements. Channel state information (CSIT) is assumed to be known at the eNodeB.

For our simulations, we assume exactly one user per sector and we do not consider any further scheduling aspects. Since no cooperation between sectors or cells is performed, the user in a specific sector is only served by the directional antennas of this sector. In our computer simulations, we consider one subcarrier (frequency-flat fading) that is modeled by Rayleigh-fading with a distance dependent pathloss and shadowing that corresponds to scenario C2 Urban NLOS Macro-Cell environment in the WINNER II channel model [4]. According to [5], this model is well suited to evaluate the performance of cooperation for LTE-Advanced. The system parameters of our simulations are summarized in Table I.

## III. COOPERATION SCHEMES

### A. Sector Cooperation

The easiest cooperation scheme is cooperation among the different sectors of one eNodeB; this leads to a multiuser MIMO approach, where one eNodeB serves multiple UEs

TABLE I  
PARAMETERS OF OUR COMPUTER SIMULATIONS.

Parameter	Value
Channel model	WINNER C2 Urban NLOS
Radius of cell	350m
Number of simulated cells	12
Carrier frequency	2.6 GHz
Frequency reuse	3
Antennas at eNodeB	4
Antenna height eNodeB	20m
Antenna gain eNodeB	17dBi
Antennas at UE	2
Antenna height UE	1.5m
Antenna gain UE	0dBi
Noise power at UE	-85 dBm

using MIMO broadcast techniques on the downlink. This is particularly simple since CSIT and transmit symbols are required only at one location, i.e. no backhaul has to be involved. The cooperation requires that all sectors use the same frequency band. In order to reduce the interference from adjacent cooperation sets, three different frequency bands are applied (frequency reuse 3). All sectors of one eNodeB use the same frequency band, neighboring eNodeBs use different frequencies. The setup is depicted in Figure 1(b).

### B. Cell Cooperation

In cell cooperation three adjacent eNodeBs will cooperate. Therefore, the frequency allocation has to be changed in a way that all three sectors of the eNodeBs forming one cooperation set will share one frequency. The antenna orientation of the eNodeBs is rotated by  $30^\circ$  in order to form the main beam towards the cooperation area. The scenario is shown in Figure 1(c).

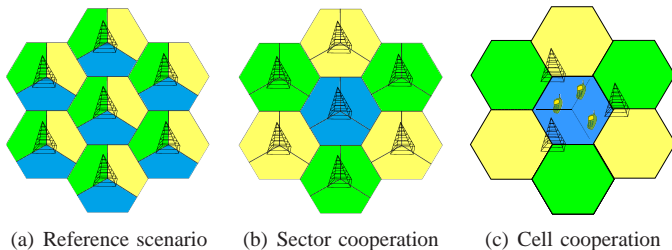


Fig. 1. Cell setup for different scenarios.

### C. Low-Power Nodes

Both the sector cooperation and the cell cooperation scheme can be extended by low-power nodes. We limit the Tx power of these additional nodes to 6W, which simplifies the deployment in some countries. Therefore, the effort in finding and setting up the site as well as in getting the official approval will be much lower. Furthermore, it can be expected that residents' acceptance of these nodes will be much higher compared to eNodeBs due to the reduced Tx power which is in the order of magnitude of private WLANs. In our investigations, we assume that the cell cooperation scheme is enhanced by three additional low power nodes that are placed at the remaining edges of the cooperation area, e.g. on a rooftop (see Figure 2). Due to the smaller size of these nodes they are assumed to

have two directional antennas compared to four antennas of eNodeBs. We distinguish three different types of low-power nodes which will be detailed in the sequel.

1) *Supporting Nodes*: Supporting nodes can also be understood as distributed antenna systems (DAS) and require backhaul links with unlimited capacity. They will strongly benefit from the macro diversity (see Figure 2). However, the realization of these supporting nodes (or remote radio heads) might be difficult and costly, especially due to the fact that the data streams have to be transmitted from eNodeBs to supporting nodes in real-time. Therefore, also other approaches without backbone have been considered.

2) *Femto Cells*: The cooperation concept for femto cells is the same as for supporting nodes: Low-power nodes are placed in the cooperation area as shown in Figure 2. The difference to supporting nodes, however, is that no backhaul is available. Therefore, data to be transmitted by the low-power nodes will in a first step be sent by eNodeBs to the low-power nodes and in a second step the received and decoded data will be forwarded by the low-power nodes to the particular UE. This means that the UE which will be served by the low-power node will only be connected to this node, i.e. cooperation between the eNodeBs only takes place to transmit data for this UE to the low-power node. In order to avoid interference between the low-power node and the eNodeBs, we assume that the transmission between low-power nodes and UEs uses another frequency band/transmission standard. This could be WiFi using the 2.4 GHz or 5 GHz frequency range. The low-power node therefore forms a locally restricted *femto cell* which is (wirelessly) connected to the eNodeBs. The advantage of this solution is that a heterogeneous network structure can easily be set up using commercial off-the-shelf WLAN equipment. However, the disadvantage is that another frequency band is required which is not exclusively reserved to the operator of the network. Therefore interferences with other (private) networks can result in reduced QoS of the network.

3) *Relay Nodes*: Finally, a cooperation scheme without backhaul and without further frequency bands has been considered. The main difference to femto cells is that in our *relay node* scheme only one frequency band is used. In order to avoid interference between low-power nodes transmitting to UEs and eNodeBs transmitting data to other UEs, the block zero-forcing algorithm described in Section IV has been extended in a way that all UEs being served by low-power nodes are considered in the optimization and interference will be cancelled out at the eNodeBs. This is possible due to the larger number of antennas at the eNodeBs in case CSIT for all UEs of the cooperation set is available. Since low-power nodes only have two antennas, this interference cancellation is not possible for UEs being served by the eNodeBs. However, since all UEs close to relay nodes will be served by them and the Tx power of these nodes is much lower compared to the Tx power of eNodeBs this amount of interference is very low, as our simulation results show.

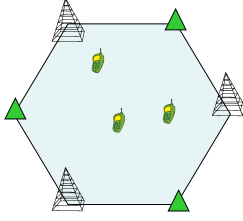


Fig. 2. Placement of additional low-power nodes (green triangles).

#### IV. COOPERATION ALGORITHM

For the explanation of our algorithm, we assume channel state information at the transmitter (CSIT), exchange of Tx symbols, and unlimited backhaul capacity between cooperating eNodeBs. A cluster of cooperating eNodeBs is referred to as a cooperation set and consists of  $M$  eNodeBs that are able to cooperate with each other in a cooperation area. The transmission within a cooperation set can be assisted by  $L$  low-power nodes (relays, femtos, or supporting nodes). These additional nodes are connected to the eNodeBs, as explained in Section III. All other transmitting nodes do not belong to this cooperation set and will cause interference.

We assume  $K = M$  UEs in our cooperation area. Each sector of an eNodeB has  $N_B = 4$  and each supporting node has  $N_S = 2$  directional antennas, with patterns as defined in [2], each UE has  $N_U = 2$  omnidirectional antennas.

In the following, the cooperation scheme in the case of supporting nodes is described. The  $M$  cooperating eNodeBs are assisted by  $L$  supporting nodes. The receive signal at UE  $k$  is

$$\mathbf{y}_k = \sum_{b=1}^M \mathbf{H}_{k,b}^{(B)} \cdot \mathbf{x}_b^{(B)} + \sum_{\ell=1}^L \mathbf{H}_{k,\ell}^{(S)} \cdot \mathbf{x}_\ell^{(S)} + \mathbf{n}_k, \quad (1)$$

where  $\mathbf{H}_{k,b}^{(B)}$  is the channel matrix of dimension  $N_U \times N_B$  describing the channel from eNodeB  $b$  in the cooperation set to UE  $k$ , and  $\mathbf{H}_{k,\ell}^{(S)}$  is the matrix describing the channel from supporting node  $\ell$  to UE  $k$ . The vectors  $\mathbf{x}_b^{(B)} \in \mathbb{C}^{N_B}$  and  $\mathbf{x}_\ell^{(S)} \in \mathbb{C}^{N_S}$  are the complex valued transmit vectors of the eNodeBs and supporting nodes, respectively. In order to keep the notation as clear as possible, we treat the *out-of-cooperation interference* as additional noise. The term  $\mathbf{n}_k$  includes therefore noise induced in the receiver as well as interference caused by the transmission of nodes outside of our cooperation set.

The I-O relation (1) can be rewritten as

$$\begin{aligned} \mathbf{y}_k &= \tilde{\mathbf{H}}_k \cdot \tilde{\mathbf{x}}_k + \tilde{\mathbf{H}}_k \sum_{j \neq k} \tilde{\mathbf{x}}_j + \mathbf{n}_k \\ &= \mathbf{y}_k^{(\text{signal})} + \mathbf{y}_k^{(\text{interference})} + \mathbf{n}_k, \end{aligned} \quad (2)$$

where  $\tilde{\mathbf{H}}_k = [\mathbf{H}_{k,1}^{(B)}, \mathbf{H}_{k,2}^{(B)}, \dots, \mathbf{H}_{k,M}^{(B)}, \mathbf{H}_{k,1}^{(S)}, \dots, \mathbf{H}_{k,L}^{(S)}]$  is the channel matrix from *all* transmitting nodes within the cooperation set to UE  $k$  and the vector  $\tilde{\mathbf{x}}_j = [\mathbf{G}_{j,1}^{(B)T}, \dots, \mathbf{G}_{j,M}^{(B)T}, \mathbf{G}_{j,1}^{(S)T}, \dots, \mathbf{G}_{j,L}^{(S)T}]^T \cdot \mathbf{s}_j$ ,  $j = 1, \dots, K$ , contains the corresponding transmit signal of the eNodeBs and supporting nodes.

Similarly to the scheme described in [3], [6], we assume linear precoding with block diagonalization. In order to completely eliminate the interference terms within the cooperation set, we decompose the precoding matrices of the eNodeBs into the product

$$\mathbf{G}_{k,b}^{(B)} = \mathbf{Z}_{k,b}^{(B)} \cdot \mathbf{Q}_{k,b}^{(B)}, \quad (3)$$

where  $\mathbf{Z}_{k,b}^{(B)}$  is a block zero-forcing matrix and  $\mathbf{Q}_{k,b}^{(B)}$  is used for power allocation of the different streams. The block zero-forcing matrices are chosen so that  $\mathbf{H}_{i,b}^{(B)} \cdot \mathbf{Z}_{j,b}^{(B)} = \mathbf{0}$ ,  $\forall i \neq j$  and  $\mathbf{Z}_{j,b}^{(B)H} \cdot \mathbf{Z}_{j,b}^{(B)} = \mathbf{I}$ . The precoding matrices of the supporting nodes are decomposed similarly. In order to fulfill these requirements, the block zero-forcing matrices  $\mathbf{Z}_{k,b}^{(B)}$  and  $\mathbf{Z}_{k,\ell}^{(S)}$  can be chosen as components of the  $N_D = M \cdot N_B + L \cdot N_S - (K - 1) \cdot N_U$  orthonormal basis vectors of the null space of  $[\tilde{\mathbf{H}}_1^T, \dots, \tilde{\mathbf{H}}_{k-1}^T, \tilde{\mathbf{H}}_{k+1}^T, \dots, \tilde{\mathbf{H}}_K^T]^T$ . The I-O relation (2) is then

$$\begin{aligned} \mathbf{y}_k &= \tilde{\mathbf{H}}_k \cdot \tilde{\mathbf{x}}_k + \underbrace{\tilde{\mathbf{H}}_k \sum_{j \neq k} \tilde{\mathbf{x}}_j}_{=\mathbf{0}} + \mathbf{n}_k \\ &= \sum_{b=1}^M \mathbf{H}_{k,b}^{(B)} \mathbf{Z}_{k,b}^{(B)} \mathbf{Q}_{k,b}^{(B)} \mathbf{s}_k + \sum_{\ell=1}^L \mathbf{H}_{k,\ell}^{(S)} \mathbf{Z}_{k,\ell}^{(S)} \mathbf{Q}_{k,\ell}^{(S)} \mathbf{s}_k + \mathbf{n}_k, \end{aligned} \quad (4)$$

where  $\mathbf{s}_k \in \mathbb{C}^{N_D}$  is the source-symbol vector intended for UE  $k$  with zero mean and variance 1. After calculating the block zero-forcing matrices which completely cancel out the interference at the receiving UEs, the matrices  $\mathbf{Q}_{k,b}^{(B)}$  and  $\mathbf{Q}_{k,\ell}^{(S)}$  have to be calculated.

According to [7], the achievable data rate can be calculated by

$$\begin{aligned} R_k &= \log_2 \det \left\{ \mathbf{K}_s^{(k)} + \mathbf{K}_i^{(k)} + \mathbf{K}_n^{(k)} \right\} - \\ &\quad \log_2 \det \left\{ \mathbf{K}_i^{(k)} + \mathbf{K}_n^{(k)} \right\}, \end{aligned} \quad (5)$$

where  $\mathbf{K}_s^{(k)} = \mathbb{E} \left\{ \mathbf{y}_k^{(\text{signal})} \cdot \mathbf{y}_k^{(\text{signal})H} \right\}$  and  $\mathbf{K}_i^{(k)}$  and  $\mathbf{K}_n^{(k)}$  are the covariance matrices of the interference and the noise with respect to user  $k$ . Due to the zero-forcing approach this simplifies to

$$R_k = \log_2 \det \left\{ \mathbf{K}_s^{(k)} + \mathbf{K}_n^{(k)} \right\} - \log_2 \det \left\{ \mathbf{K}_n^{(k)} \right\}. \quad (6)$$

The goal of the optimization is to determine the matrices  $\mathbf{Q}_{k,b}$  while the per-node power constraints

$$\text{Tr} \left\{ \mathbf{x}_b^{(B)} \cdot \mathbf{x}_b^{(B)H} \right\} = \text{Tr} \left\{ \sum_{j=1}^K \mathbf{Z}_{j,b}^{(B)} \mathbf{Q}_{j,b}^{(B)} \mathbf{Q}_{j,b}^{(B)H} \mathbf{Z}_{j,b}^{(B)H} \right\} \leq P_B, \quad (7)$$

and

$$\text{Tr} \left\{ \mathbf{x}_\ell^{(S)} \cdot \mathbf{x}_\ell^{(S)H} \right\} = \text{Tr} \left\{ \sum_{j=1}^K \mathbf{Z}_{j,\ell}^{(S)} \mathbf{Q}_{j,\ell}^{(S)} \mathbf{Q}_{j,\ell}^{(S)H} \mathbf{Z}_{j,\ell}^{(S)H} \right\} \leq P_S, \quad (8)$$

must not be violated  $\forall b \in \{1, \dots, M\}$  and  $\forall \ell \in \{1, \dots, L\}$ .

In our investigations, we consider two different optimization approaches:

- *Peak Power Minimization*

Our first optimization approach is to minimize the maximum sum power of one sector (i.e. sum of the  $N_B$  antenna elements). This approach has large practical relevance in order to minimize electromagnetic radiation and the out-of-cooperation interference. Minimizing the maximum power results in equal power distribution over all  $M$  cooperating sites. In order to achieve fairness between the users, we define a minimum target rate which has to be achieved by all users in the cooperation set.

- *Data Rate Maximization*

In our second optimization approach, the goal is to maximize the data rate within the cooperation set. Applying a sum data rate constraint for all users in the cooperation set could result in an imbalanced share of data rates between the users, e.g. a user at the cell edge could get a very low data rate and users close to the eNodeB would get a very high data rate. To achieve fairness between the users, we use a max-min-constraint which means the minimum data rate over the users in our cooperation set is maximized. This results in equal data rates of all  $K$  users within our cooperation area. In this scenario the Tx power is fixed to typical values.

For each approach the optimal matrices  $\mathbf{Q}_{k,b}$  can be found by numerical optimizations. Both approaches described above, however, are suboptimal for three reasons:

- 1) Cooperation is restricted to eNodeBs of one cooperation set.
- 2) Interference generated from eNodeBs outside of this cooperation set is generally not known and hence ignored in the optimization of  $\mathbf{Q}_{k,b}$ . However, the effect of this interference on the achievable rates is taken into account in our simulations.
- 3) The block zero forcing approach is an heuristic approach to achieve optimality in our simulations.

Nevertheless, both schemes are simple, easy to implement, and, hence, of high practical relevance. The resulting min-max-optimization/max-min-optimization problems are convex/concave, respectively [8]. Therefore, the optimization problem for the determination of matrices  $\mathbf{Q}_{k,b}$  can be efficiently solved by standard optimization tools like e.g. the Yalmip Toolbox [9].

## V. RESULTS

Our simulation environment considers all discussed cooperation schemes. Per sector, exactly one user is assumed at a random position. For UEs in the coverage range of a femto cell or a relay node both options of connection, i.e. directly served by eNodeBs or connected through low-power node, are considered and the option resulting in lowest peak Tx power or highest minimum data rate, respectively, is chosen. Therefore an exhaustive search is performed to consider all possible options. Low-power nodes are assumed to be mounted at a height of 5m above ground and for the connection between eNodeBs and femto cells or relay nodes,

respectively, a line-of-sight channel model is used. Adjacent cells are considered as interferers transmitting with Tx power of 80W. The number of simulations per scheme was 20000. Results for both optimization approaches are discussed in the following subsections.

### A. Peak Power Minimization

For the minimization of Tx power we define a target data rate of 1 bit/s/Hz which has to be achieved by all users in the cooperation set. The maximum Tx power  $P_S$  of a low-power node is limited to  $\min\{6W, P_B^*\}$ , where  $P_B^*$  is the maximum Tx Power of the eNodeBs after the optimization. Without this min-max-condition, the optimization often leads to the contrary of our optimization goal, namely that the low power nodes have to transmit with their maximum power and the Tx power of eNodeBs is minimized below the low-power node Tx limit. The simulation results are shown in Figure 3.

For the reference scenario, the cumulative distribution function (CDF) shows the distribution of the maximum transmission power from the three sectors, i.e.  $\max\{P_{B, \text{Sector 1}}^*, P_{B, \text{Sector 2}}^*, P_{B, \text{Sector 3}}^*\}$ . It can be seen that using a peak power value  $P_B$  of 49dBm (80W) the target rate of 1 bit/s/Hz can be achieved only in about 47% of our simulations whereas for the supporting nodes scheme it can be achieved in about 97%. Femto cells and relay nodes have approximately the same performance. This shows that the amount of interference caused by relay nodes is almost negligible. A large difference between sector cooperation and cell cooperation can be observed due to two main reasons:

- 1) The antenna beam pattern of [2] is not optimal in case of sector cooperation since it spatially separates large parts of the cooperation area. It is therefore better suited for cell cooperation.
- 2) Cell cooperation benefits from macro diversity gains due to the different eNodeB locations.

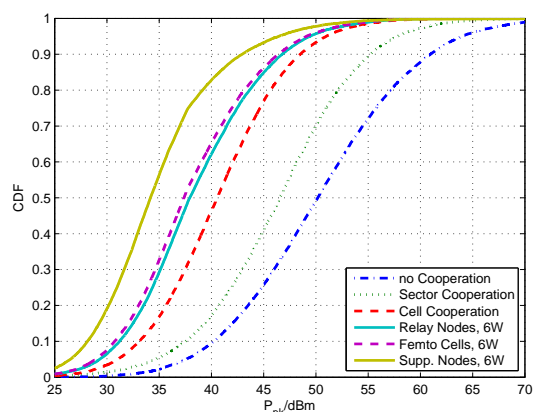


Fig. 3. CDF of peak power for all considered cooperation schemes to achieve min. rate of 1 bit/s/Hz.

### B. Data Rate Maximization

Despite Tx power reduction, the maximum data rate that can be achieved with these schemes is also of interest for operators of mobile networks. Therefore we fixed the Tx power of

eNodeBs and low-power nodes to typical peak power values of  $P_B=80\text{W}$  [2] and  $P_S=6\text{W}$ , respectively. For the simulations we assumed independent and locally restricted cooperation sets. This means that CSIT from interfering cooperation sets is not available and cannot be considered in the optimization. However, interference caused by adjacent cooperation sets will lower the data rate and therefore has been considered in our simulation environment. Figure 4 shows the CDF of the minimum data rate within the cooperation set. Again, the reference scenario and the sector cooperation scenario are clearly outperformed by the other cooperation schemes. Supporting nodes achieve highest data rates while the relay node scheme and the femto cell scheme perform very similar with only minor improvement compared to cell cooperation without additional low-power nodes.

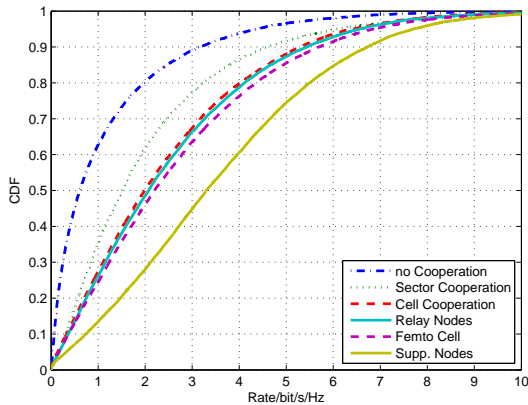


Fig. 4. CDF of data rates achieved with a eNodeB Tx power of 80W and low-power node Tx power of 6W.

### C. Limitation of Backhaul Capacity

Supporting nodes seem to be an appealing solution to achieve high data rates and low Tx power. However, up to here we assumed unlimited backhaul capacity which will hardly be available in practical networks. Therefore a limitation of backhaul capacity for the link between eNodeBs and supporting nodes has been investigated, assuming a bandwidth of 100 MHz on the wireless channel being used by the cooperation set. The supporting node scheme requires a backhaul capacity between eNodesBs and low-power nodes of  $K \cdot R \cdot BW$ , where  $K$  is the number of users,  $R$  the rate in bit/s/Hz achieved by the users, and  $BW$  the bandwidth on the wireless channel. Our simulation results of cell cooperation and supporting node schemes deliver the data rates without backhaul and with unlimited backhaul, respectively. In case of backhaul limitation we use the data rate of cell cooperation as baseline and estimate the data rate increase achieved with supporting nodes by linear interpolation. It is obvious that this is only a theoretical limit, neglecting all implementation aspects. Despite of this, it gives good insights on backhaul capacity requirements. The results of our simulations are shown in Figure 5. It turns out that for reasonable performance increase, which can justify the effort of enhancing the network by low-power nodes, a backhaul capacity of more than 1 Gbps is recommended for the considered setup.

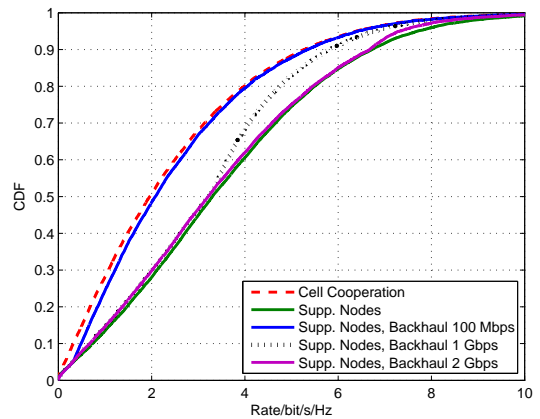


Fig. 5. Investigation of limited backhaul for supporting nodes. Minimum rate for bandwidth of 100 MHz,  $P_B = 80\text{W}$ ,  $P_S = 6\text{W}$ .

## VI. CONCLUSION

Different cooperation schemes for the downlink of next generation mobile networks have been investigated by means of simulations and discussed with respect to peak Tx power, achievable data rate, and implementation issues. The focus of our investigations has been on simple and efficient algorithms which are easy to implement and thus have a high level of practical relevance. Our results show that power reduction or data rate increase is possible by a large scale, also in case of simple and easy to implement cooperation schemes. Best performance is achieved by supporting nodes. However, for reasonable performance increase, a backhaul with very high capacity is required. From a practical point of view, a promising and feasible approach is to apply cell cooperation which could be enhanced by relay nodes and femto cells. Both enhancements provide almost similar performance and can decrease Tx power requirements in a wide range.

## REFERENCES

- [1] Radiocommunication sector of ITU, ITU-R, "Framework and overall objectives of the future development of IMT-2000 and systems beyond IMT-2000," *Recommendation ITU-R M.1645*, June 2003.
- [2] 3rd Generation Partnership Project 3GPP, "Further advancements for E-UTRA physical layer aspects (release 9)," *3GPP TR 36.814, V9.0.0*, March 2010.
- [3] M. Kuhn, R. Rolny, A. Wittneben, M. Kuhn, and T. Zaslowski, "The potential of restricted PHY cooperation for the downlink of LTE-advanced," *Proceedings IEEE International Conference on Vehicular Technology, VTC Fall*, 2011.
- [4] P. Kyösti *et al.*, "WINNER II channel models," WINNER, Tech. Rep. IST-4-027756 WINNER II D1.1.2 V1.2 Part I Channel Models, Sep. 2007.
- [5] C.-X. Wang, X. Hong, X. Ge, X. Cheng, G. Zhang, and J. Thompson, "Cooperative MIMO channel models: A survey," *Communications Magazine, IEEE*, vol. 48, no. 2, pp. 80–87, February 2010.
- [6] N. Ravindran and N. Jindal, "Mimo broadcast channels with block diagonalization and finite rate feedback," *CoRR*, vol. abs/cs/0610077, 2006.
- [7] D. Tse and P. Viswanath, *Fundamentals of wireless communication*, 1st ed. Cambridge, UK: Cambridge University Press, 2005.
- [8] M. K. Karakayali, G. J. Foschini, R. A. Valenzuela, and R. Yates, "On the maximum common rate achievable in a coordinated network," in *IEEE International Conference on Communications, ICC2006*, June 2006.
- [9] J. Löfberg, "Yalmip: A toolbox for modeling and optimization in matlab," in *CACSD Conference, Taipei, Taiwan*, 2004.